

Study of the prediction model of water flux through a forward osmosis membrane

Issa Ndiaye^{a,*}, Imane Chaoui^{a,b}, Sébastien Vaudreuil^a, Tijani Bounahmidi^a

^aEuro-Med Research Institute, Euro-Med University of Fes (UEMF), Rond-point Bensouda Route Nationale de Meknès, BP 51 Fes (Morocco), emails: i.ndiaye@ueuromed.org (I. Ndiaye), i.chaoui@ueuromed.org (I. Chaoui), s.vaudreuil@ueuromed.org (S. Vaudreuil), t.bounahmidi@ueuromed.org (T. Bounahmidi)

^bEcole Mohammadia d'Ingénieurs, Université Mohamed V-Rabat, Avenue Ibn Sina B.P 765, Agdal Rabat (Morocco)

Received 20 May 2021; Accepted 27 October 2021

ABSTRACT

This work aims at evaluating the accuracy of Tiraferri's model introduced in 2013 for predicting water flux through the forward osmosis (FO) membrane. To this end, a database of FO membranes with their intrinsic parameters and experimental water fluxes was thus constituted. The model was solved numerically in Python Software, first by considering the contribution of external concentration polarization (ECP), and by neglecting it. Using the pressure retarded osmosis mode model, the mass transfer coefficient was adjusted to fit the experimental data to the transport equation. The predicted water fluxes are mostly in agreement with the experimental data, with a resulting mean absolute error (MAE) of 9.18%. This study also shows that the error caused by ECP is less than 1% when deionized water is used as feed solution in FO mode. Because of the reverse salt flux, the ECP was found higher when membranes with high water or salt permeability are tested. The error in van't Hoff prediction, from which the model is based, was found to be low when the draw solution has a concentration in the range of 1 to 2.3 M. Some of the studied membranes exhibit however high MAE, possibly explained by errors from van't Hoff prediction or errors in the membrane parameters. This latter source of error was not accounted for in this study.

Keywords: Forward osmosis; Modelling; Membranes

1. Introduction

Recent years have seen renewed interest in forward osmosis (FO) for water treatment and purification due to its potential to reduce the energy bill [1]. FO process rely on the difference in osmotic pressure across a semi-permeable membrane to induce a flow of water from a solution with a low concentration of solute (feed solution or FS) to a high concentration solution (draw solution) [2–4]. The draw solution (DS) is subsequently separated from the permeate to be reused [5]. While the FO process operates using a thermolytic DS, low-grade energy is required in the regeneration stage [6].

While the performance of a FO membrane is characterized by its water flux (J_w) and reverse salt flux (J_s or RSF), the performance of a FO system will depend on diverse criteria. Among those are the properties of the membranes used, the physical properties of FS and DS (osmotic pressures, solute diffusivity), the operating conditions (temperature, cross-flow velocity) and the FO module configuration, etc. This FO membrane can be either asymmetrical, having a dense part underneath a porous one, or composite, having a selective/active layer over a support layer (Fig. 1). Three distinct parameters serve to characterize the FO membrane which is the water permeability "A", solute permeability "B" and structural parameter "S" [2,7]. At least two distinct methods can

* Corresponding author.

be used to determine the membrane parameters. The most used is a two-step process that involves both reverse osmosis (RO) and FO tests [8,9]. The factors determining the FO system performance are themselves measured experimentally through FO tests [10].

Mathematical modeling is nowadays a good strategy to evaluate the performance of FO systems. It allows system visualization and a better understanding of its behavior. It also highlights the effects of various parameters on the system, which can help in designing the FO membrane and optimizing the operating conditions.

The present work focuses on water flux modeling. The mass transfer through an FO membrane was described through physical and semi-empirical models for a long period [11]. Tiraferri et al. [7] proposed a method for the simultaneous determination of the A , B and S parameters of FO membranes. This method consists of fitting the FO transport models to experimental water and salt fluxes. To this end, they developed a new model describing the water flux through FO membranes, which was inspired by Yip et al.'s work [12]. Since its introduction, few works in the literature have addressed the accuracy of this model. It is thus essential to evaluate it in various operating conditions and different membranes.

This work thus aims at studying the accuracy of this model. A database of FO membranes was constituted from available scientific research, which includes the intrinsic parameters of membranes, experimental water fluxes, etc. The mathematical model is solved iteratively on Python Software using the "Levenberg–Marquardt (LM)" algorithm integrated into the scipy optimize package. The predicted water fluxes are compared afterward with experimental data.

2. Water flux modeling

The general equation of the water flux through an FO membrane is given by the following [13]:

$$J_w = A(\sigma\Delta\pi - \Delta P) \quad (1)$$

where J_w is the water flux (in m/s); A is the water permeability of the membrane (m/s Pa); σ is the reflection coefficient; $\Delta\pi$ represents the difference in osmotic pressure (in Pa) between the FS and DS solutions and ΔP is the applied pressure (in Pa).

The reflection coefficient takes into account the back diffusion of solutes across the membrane. σ value of 0 means that solutes cannot be retained by the membrane, whereas a complete rejection of solutes yields a value of 1. The water flux given by Eq. (1) is however theoretical. In practice, the water flux is affected by the concentration polarization (CP) phenomena occurring in the FO process, which reduces the osmotic pressure across the membrane selective layer (Fig. 1).

The CP phenomena can be either internal concentration polarization (ICP) when it takes place within the support layer, or external concentration polarization (ECP) when it occurs on the active layer side [1,13,14]. CP can be considered dilutive when it induces dilution of the DS, whereas concentrative CP is the accumulation of solutes on the membrane surface. The presence of this CP reduces the osmotic pressure gradient across the membrane, resulting in lower water flux. This will be influenced by the operating mode of the FO membrane. In FO mode, the active layer of the membrane will face the FS but will face the DS instead when operating in pressure retarded osmosis (PRO) mode. It is known that ECP has less effect on the water flux than ICP when the membrane is in FO mode [15].

The model studied is established using the mass transfer equations of solutes across the membrane [7] and van't Hoff's equation [Eq. (2)] which expresses a linear relationship between the osmotic pressure and the concentration. The semi-empirical model in FO mode is given by Eq. (3) [7]:

$$\pi = i C R T \quad (2)$$

$$J_w = A \left\{ \frac{\pi_{D,b} \exp\left(-\left(\frac{J_w S}{D}\right)\right) - \pi_{F,b} \exp\left(\frac{J_w}{k}\right)}{1 + \left(\frac{B}{J_w}\right) \left[\exp\left(\frac{J_w}{k}\right) - \exp\left(-\frac{J_w S}{D}\right) \right]} \right\} \quad (3)$$

where k is the mass transfer coefficient defined as the ratio between the solute diffusivity (D) and the thickness of the boundary layer (δ) (Fig. 1), resulting in the accumulation of solutes on the membrane surface; S takes into consideration the impact of the support layer structure on the water flux.

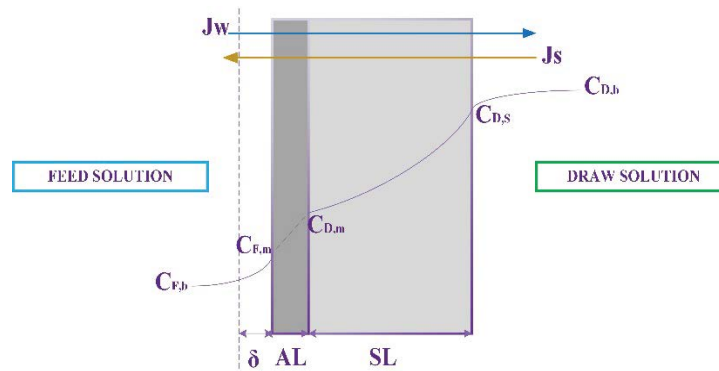


Fig. 1. Concentration profile across an FO mode-oriented membrane.

In this model, the terms “ $\exp\left(\frac{J_w}{k}\right)$ ” and “ $\exp\left(\frac{J_w S}{D}\right)$ ” take into account the concentrative ECP and dilutive ICP, respectively, while the term “ $1 + \frac{B}{J_w} \left[\exp\left(\frac{J_w}{k}\right) - \exp\left(-\left(\frac{J_w S}{D}\right)\right) \right]$ ” represents the reflection coefficient of the solutes σ . The degree of ICP for a membrane can be appreciated via the structural parameter, with lower S values yielding lower ICP [11]. The FO membrane should thus be designed to minimize the S value to mitigate ICP.

S is expressed as a function of the tortuosity (τ), porosity (ϵ) and thickness (δ) of membranes as follows.

$$S = \frac{\tau \delta}{\epsilon} \quad (4)$$

The water flux prediction model for the PRO mode is described as follows [12]:

$$J_w = A \left\{ \frac{\pi_{D,b} \exp\left(-\left(\frac{J_w}{k}\right)\right) - \left(\pi_{F,b} \exp\left(\frac{J_w S}{D}\right)\right)}{1 + \left(\frac{B}{J_w}\right) \left[\exp\left(\frac{J_w S}{D}\right) - \exp\left(-\left(\frac{J_w}{k}\right)\right) \right]} - \Delta P \right\} \quad (5)$$

3. Database and methodology

3.1. Determination of membrane parameters and experimental water flux

The intrinsic water permeability A and the solute permeability B of FO membranes are generally established using a RO system. The pure water flux $J_{w_{RO}}$ is then calculated by dividing the volumetric permeate rate by the membrane surface. Water permeability and solute rejection (R) are calculated from the following expressions [10]:

$$J_{w_{RO}} = \frac{\Delta V}{\Delta t A_m} \quad (6)$$

$$A = \frac{J_{w_{RO}}}{\Delta P} \quad (7)$$

$$R = \left(1 - \frac{C_p}{C_f} \right) \times 100\% \quad (8)$$

where C_p and C_f are the concentrations of solutes in permeate and feed, respectively, which can be determined by simple electrical conductivity measurement. R coefficient defines the amount of solutes in the feed solution that is not able to cross the semipermeable membrane.

Solute permeability is calculated based on the solution-diffusion theory according to Eq. (9) [16]:

$$B = J_{w_{RO}} \left(\frac{1-R}{R} \right) \exp\left(-\frac{J_{w_{RO}}}{k}\right) \quad (9)$$

The structural parameter is determined using a FO system and the classical model of ICP described by Eqs. (10)

and (11) in PRO mode and FO mode, respectively [17]. The $J_{w_{FO}}$ is calculated as in Eq. (7).

$$J_{w_{FO}} = \frac{D}{S} \left[\ln \frac{A \cdot \pi_D - J_v + B}{A \cdot \pi_F + B} \right] \quad (10)$$

$$J_{w_{FO}} = \frac{D}{S} \left[\ln \frac{A \cdot \pi_D + B}{A \cdot \pi_F + J_v + B} \right] \quad (11)$$

3.2. Database and calculation of fluid properties

To perform this study, 10 R&D membranes available in the literature were selected. The water flux of these membranes was calculated using the model described by Eq. (4), while respecting the experimental testing conditions summarized in Table 1.

In all studied experiments, NaCl and deionized (DI) water are used as DS and FS, respectively. The osmotic pressure is calculated using Eq. (5) which describes a non-linear relationship between the osmotic pressure and concentration of NaCl [26]. This relationship is obtained from fitting the simulated data in OLI STREAM software for a temperature of 25°C.

$$\pi = 3.805 \times C^2 + 42.527 \times C + 0.434 \quad (12)$$

The diffusivity coefficient was estimated using the following [26]:

$$D = -1.025 \times 10^{-10} \times C + 1.518 \times 10^{-9} \quad (13)$$

The mass transfer coefficient “ k ” is dependent on the characteristics of the test cell (length, width, etc.), operating conditions (crossflow velocity, temperature, etc.), solution properties (viscosity, solute diffusivity), etc. [27]. Since the mass transfer coefficient or dimensions of the test cells are not always available in the literature, k is determined using the water flux model in PRO mode [Eq. (5)]. The objective is to adjust k to fit the PRO transport equation to the experimental data [10].

3.3. Model calculation in Python

To calculate the FO water flux, the model was implemented in Python Software using the LM algorithm [28] integrated in scipy optimize package [29]. This algorithm allows solving the model by iteration. LM has the advantage of taking less time to converge [30]. To reduce the convergence time, it is important to take an initial value close to the expected solution. To deal with this, the experimental water flux is given as the initial value. The solving procedure involves first calculating the osmotic pressure and diffusivity of the DS using Eqs. (13) and (14), respectively, taking into account concentration. The values obtained for diffusivity and osmotic pressure, as well as the mass transfer coefficient and intrinsic parameters of the membranes, are given as input parameters for the model which is then solved the iterative procedure implemented in Python is presented in Fig. 2. The model accuracy is evaluated by comparing the predicted water fluxes and the experimental data.

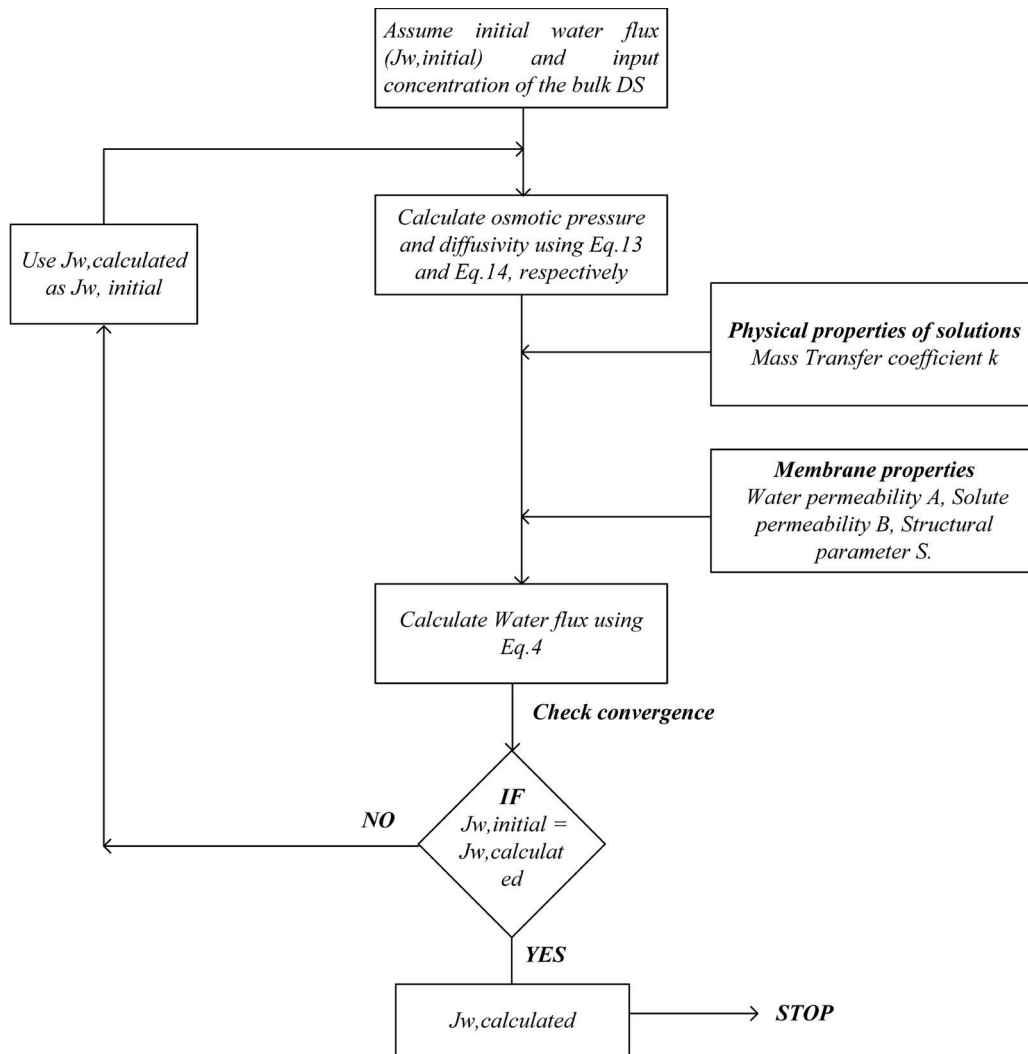


Fig. 2. Iteration procedures implemented in Python Software.

4. Results and discussion

4.1. Water flux neglecting ECP

The water flux was first predicted by assuming that ECP did not occur at the membrane surface, since DI water is used as FS. Tiraferri et al. [7] neglected ECP since the built-up of solutes at the active layer surface could be avoided as they used DI water as FS. The solute back diffusion is also assumed minimal to induce ECP. ECP can be minimized by increasing turbulence at the membrane surface [13].

The predicted and experimental water fluxes of membranes are summarized in Table 2. For each membrane, the water flux and error experimental (standard deviation) are given for each considered DS concentration. The model is considered as accurate when the difference between the experimental and predicted water flux is less than the experimental error.

The results summarized in Table 2 show that predicted water fluxes fit mostly with the experimental fluxes, a mean absolute error (MAE) of 9.18% being obtained when considering all of the studied membranes. Increasing the DS

Table 1 Database of membranes

Membranes	A (LMH/bar)	B (LMH)	S (µm)	Reference
M1	1.65	0.12	167	[10]
M2	1.61	0.20	241	[10]
M3	2.97	0.39	334.6	[18]
M4	0.43	0.05	210	[19]
M5	0.52	0.09	630	[20]
M6	3.03	2.92	2090	[21]
M7	1.25	0.54	392	[22]
M8	1.47	0.278	168	[23]
M9	7.6	0.5	172	[24]
M10	3.16	0.55	553	[25]

concentration leads to improved water flux as the osmotic pressure gradient across the membrane is the driving force responsible for water transport. The results also reveal that the model predicts the water flux with sufficient

Table 2
Comparison of experimental and predicted water fluxes when ECP is neglected

Membranes	DS concentration (M)	Experimental water flux ($J_{w_{EXP}}$) (LMH)	Predicted water flux $J_{w_{noECP}}$ (LMH)	$\frac{ J_{w_{noECP}} - J_{w_{EXP}} }{J_{w_{EXP}}}$	MAE (%)	Model accuracy
M1	0.5	20 ± 1	20.113	0.565%	3.42%	accurate
	1	30 ± 1	30.3	1.000%		accurate
	2	42 ± 1	43.32	3.143%		not accurate
	3	55 ± 1	52.283	4.940%		not accurate
	4	64 ± 1.5	59.241	7.436%		not accurate
M2	0.5	18 ± 2	17.045	5.306%	4.3%	accurate
	1	25 ± 2	24.846	0.616%		accurate
	2	37 ± 2.5	34.503	6.749%		accurate
	3	44 ± 2	41.021	6.770%		not accurate
M3	4	47 ± 2.5	46.029	2.066%	14.11%	accurate
	0.5	–17.5	19.735	12.77%		–
	1	25 ± 5	26.611	6.44%		accurate
	2	40 ± 2.5	34.588	13.53%		not accurate
M4	3	48 ± 5	39.761	17.17%	9.04%	not accurate
	4	55 ± 1.5	43.649	20.64%		not accurate
	0.3	6	4.825	19.58%		–
M5	1	13 ± 1.5	12.418	4.48%	12.87%	accurate
	1.5	17 ± 2	16.481	3.05%		accurate
M6	0.1	2 ± 0.5	1.945	2.75%	7.11%	accurate
	0.5	5	5.9042	18.08%		–
	1	7.5 ± 2	8.7496	16.66%		accurate
M7	1.5	12.5	10.752	13.98%	3.88%	–
	1	7.5 ± 2.25	6.9668	7.11%		accurate
M8	2	24 ± 2.5	23.07	3.88%	6.34%	accurate
	0.25	14 ± 4	11.557	17.45%		accurate
	0.5	17.5 ± 1.5	18.623	6.42%		accurate
M9	1	28 ± 5	28.388	1.39%	17.34%	accurate
	2	41	41.018	0.044%		accurate
	0.25	27 ± 2	31.503	16.68%		not accurate
	0.5	37 ± 2	43.373	17.22%		not accurate
M10	1	50 ± 2	57.335	14.67%	9.42%	not accurate
	1.5	55 ± 1	66.436	20.79%		not accurate
			MAE	9.18%		

accuracy for most of the studied membranes. Only M1, M3 and M9 membranes are exceptions to this trend, with MAE of 3.41%, 14.11% and 17.34% respectively obtained.

For M1 and M3 membranes, the model is accurate in predicting the water flux only when the DS concentration is below 2 M. In the case of the M9 membrane, the predicted water fluxes do not match the experimental values for any concentration between 0.25 and 1.5 M. A comparison of the predicted and experimental water fluxes for M1 and M9 is presented in Fig. 3.

The error in model prediction could be attributed to an ECP caused by RSF, as M1 and M3 membranes do not fully reject solutes. RSF is driven by the diffusive flux of solutes induced by the concentration gradient across the

membrane and the convective flux of solutes due to water molecule's transport across the membrane. RSF may be more significant for M1 and M3 given that higher DS concentrations are used, resulting in a high RSF. It is worth noting that DS concentrations lower than 2 M are also involved for all other membranes. Under these conditions, the reduced concentration gradient across the membranes yields however a lower diffusive flux. Membranes having low salt permeability like M4 and M5 are further subject to a minimal RSF. When DI-based FS are used, ECP may be neglected either if low DS concentration and highly selective membranes are implemented, or if membranes with low water permeability are tested. In the case of M9, a high RSF may be linked to a dominant convective flux

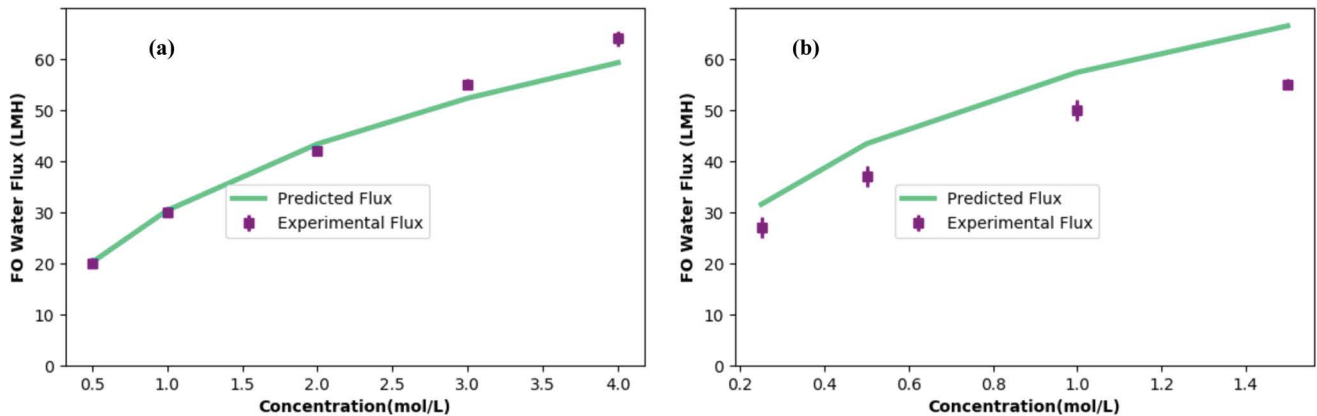


Fig. 3. Comparison of predicted and experimental water fluxes: (a) M1 membrane and (b) M9 membrane.

linked to the high water permeability of the membrane of 7.6 LMH/bar. Despite that the flux prediction for M5 and M8 are accurate, the obtained MAE remains however high due to the high experimental error. The mean error associated with the van't Hoff prediction could explain the high MAE obtained for some membranes. As illustrated in Fig. 4, the error from van't Hoff predictions for the osmotic pressure is found to exceed 5% when concentrations are between 0.5 to 1 M, or greater than 2.3 M. This error will exceed 10% for DS concentration above 2.9 M. To achieve a minimal error caused by van't Hoff predictions, a DS concentration in the 1 to 2.3 M a range of should be applied. The data obtained from OLI STREAM meet those predicted using the van't Hoff equation at the 1.6 M concentration. It is well known that van't Hoff relationship is solely applicable for very dilute solutions [31].

Low MAE values are obtained for M1 and M2 even at high DS concentrations. The high MAE obtained for some membranes may therefore be associated with the measurements of membrane parameters, especially the structural parameter where its value depends on operating conditions [4]. Given the above considerations, it will be necessary to evaluate the impact of ECP on water flux for those membranes for which the model does not accurately predict the water flux.

4.2. Water flux considering ECP

The mass transfer coefficient was adjusted to minimize the variance between experimental data and the predicted values by the model in PRO mode [Eq. (5)]. The coefficient of determination, or R -squared (R^2), which indicates how well the model fits the experimental data, was subsequently determined. The optimal k values achieved R^2 values higher than 0.90. The PRO prediction model was used since RSF is more significant in PRO mode than in FO mode. The membrane is, therefore, more prone to ECP when operated in PRO mode. The lower ICP in PRO mode also promotes a high water flux, which can induce a more severe ECP [32].

Table 3 reports the predicted water fluxes in FO mode for M1, M2, M4, M5 and M9 membranes when ECP is considered and neglected. Results show respective MAE of 3.41%, 4.34%, 9.13%, 12.86% and 16.85% when ECP is accounted for. These values are very similar to those

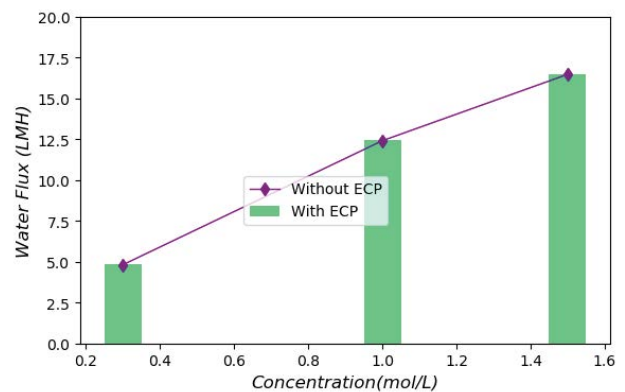


Fig. 4. Evolution of the error due to van't Hoff for osmotic pressure prediction as a function of concentration.

obtained when ECP is not considered (Table 2), with differences ranging from 0.07% to 0.49%. This indicates that ECP has less influence on the water flux when the membrane is oriented in FO mode. The low impact of ECP could be attributed to the fact that DI water is used as FS and combined with FO membranes subjected to weak RSF in test conditions. As mentioned earlier, the contribution of ECP in reducing water flux in FO mode is far smaller compared to that of ICP. For M9, the impact of ECP on water flux is not negligible due to the significant convective flux of solutes with the high permeability associated with this membrane, as already assumed in the previous section. This highlights the fact that ECP cannot be neglected when electrolytic FS are used. ECP has however a very low impact on the M4 membrane, which exhibits a low boundary layer thickness resulting in a high mass transfer coefficient of 10^{-3} . Because DI water is used as FS, ECP can only come from the reverse diffusion of solutes. Since M4 has a low permeability to solutes (0.05 LMH), it is very unlikely to be sensitive to ECP as shown in Fig. 5.

To evaluate the relationship between ECP and DS concentration, the difference between $J_{w_{ECP}}$ and $J_{w_{noECP}}$ was weighted by the average $J_{w_{ECP}}$ of membranes to account for the different orders of magnitude of $J_{w_{ECP}}$. It can be observed that increasing the DS concentration results in increased weighed difference for all selected membranes. Increased

Table 3
Evaluation of the contribution of ECP in FO mode

Membranes	DS concentration (M)	$J_{w_{PRO}}$ (LMH)	$k \times 10^{-5}$ (m/s)	$J_{w_{ECP}}$ (LMH)	$\frac{ J_{w_ECP} - J_{w_{EXP}} }{J_{w_{EXP}}}$	MAE (%)	Difference in MAE	$\frac{ J_{w_ECP} - J_{w_{no_ECP}} }{\sum_{i=1}^n J_{w_ECP}}$
M1	0.5	33 ± 1	6.5 ^a	20.106	0.53%	3.41%	0.013%	0.017%
	1	59 ± 1		30.292	0.97%			0.019%
	2	100 ± 2		43.310	3.12%			0.024%
	3	132 ± 1		52.272	4.96%			0.027%
	4	157.5 ± 1		59.229	7.45%			0.029%
M2	0.5	30 ± 1	6.5 ^a	17.036	5.36%	4.34%	0.039%	0.028%
	1	52.5 ± 1		24.835	0.66%			0.034%
	2	85 ± 1		34.491	6.78%			0.037%
	3	105 ± 1.5		41.008	6.80%			0.040%
	4	112.5 ± 1		46.015	2.10%			0.043%
M4	0.3	7 ± 1	102	4.818	19.70%	9.13%	0.095%	0.062%
	1	21.5 ± 2.25		12.406	4.57%			0.107%
	1.5	28 ± 2		16.467	3.14%			0.125%
M5	0.1	2.5 ± 1	10.5	1.949	2.55%	12.86%	0.007%	0.058%
	0.5	7.5 ± 1		5.911	18.22%			0.099%
	1	12.5 ± 3.5		8.756	16.75%			0.094%
	1.5	22 ± 1		10.758	13.94%			0.088%
M9	0.25	42 ± 2	1.9	31.358	16.14%	16.85%	0.49%	0.293%
	0.5	65 ± 2.5		43.189	16.73%			0.372%
	1	91 ± 5		57.106	14.21%			0.463%
	1.5	108 ± 2		66.176	20.32%			0.526%

^ak value experimentally determined [10]; $J_{w_{ECP}}$: predicted water flux considering ECP; $J_{w_{noECP}}$: predicted water flux without ECP; $J_{w_{PRO}}$: experimental water flux in mode PRO. $J_{w_{ECP}}$ and $J_{w_{EXP}}$ are given in Table 1.

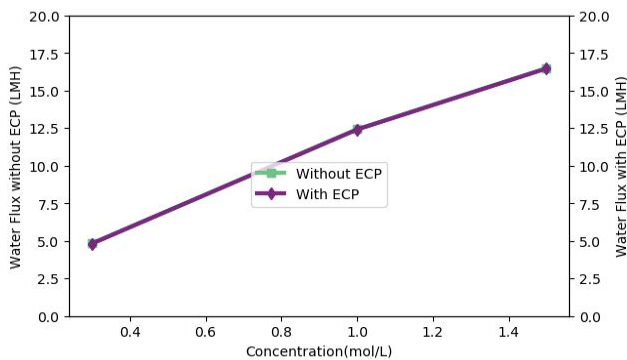


Fig. 5. Comparison of predicted water fluxes with or without considering ECP for M4.

RSF severity with concentration could explain this, as higher gradient concentrations through the membrane are responsible for the flux of solutes.

It is worth noting however that inaccuracy of the model cannot be attributed to ECP given its small impact on the water flux. Errors in measuring membrane parameters, not accounted for in this study, could explain the high MAE obtained for some membranes.

5. Conclusion

The FO model for water flux was coded in python using the LM algorithm integrated in the scipy-optimize package. The water flux was predicted for 10 R&D membranes and the results were compared with experimental data. The results show that the FO model is good at predicting the water flux of membranes, having an MAE of 9.18% against experimental data. This work revealed that ECP influences the water flux less when the membrane operates in FO mode, especially when DI water is used as FS. High water permeability and high solute permeability membranes are, however, vulnerable to RSF where the effects of ECP can be exacerbated when even highly dilute FS are tested. It was found that the error caused by ECP increases with DS concentration, but values lower than 1% can however be achieved. The error attributed to the van't Hoff prediction was found at its lowest for DS concentrations between 1 to 2.3 M. High MAE were observed for some membranes that could be attributed either to van't Hoff predictions, or to errors in measuring membrane parameters. This study does not however account for such error in measurements. It would be important to progress towards models that consider the non-linear relationship between concentration and osmotic pressure to give better predictions. Another challenge would also be to find methods

that reduce the error associated with the determination of membrane parameters.

Acknowledgments

The authors acknowledge the financial support from Euro-Med University of Fes (UEMF).

References

- [1] C. Klaysom, T.Y. Cath, T. Depuydt, I.F.J. Vankelecom, Forward and pressure retarded osmosis: potential solutions for global challenges in energy and water supply, *Chem. Soc. Rev.*, 42 (2013) 6959–6989.
- [2] I. Ndiaye, S. Vaudreuil, T. Bounahmidi, Forward osmosis process: state-of-the-art of membranes, *Sep. Purif. Rev.*, 50 (2021) 53–73.
- [3] I. Chaoui, I. Ndiaye, S. Abderafi, S. Vaudreuil, T. Bounahmidi, Evaluation of FO membranes performance using a modelling approach, *Desal. Water Treat.*, 223 (2021) 71–98.
- [4] I. Ndiaye, I. Chaoui, S. Vaudreuil, T. Bounahmidi, Selection of substrate manufacturing techniques of polyamine-based thin-film composite membranes for forward osmosis process, *Polym. Eng. Sci.*, 61 (2021) 1912–1930.
- [5] I. Chaoui, S. Abderafi, S. Vaudreuil, T. Bounahmidi, Water desalination by forward osmosis: draw solutes and recovery methods – review, *Environ. Technol. Rev.*, 8 (2019) 25–46.
- [6] R.L. McGinnis, M. Elimelech, Energy requirements of ammonia-carbon dioxide forward osmosis desalination, *Desalination*, 207 (2007) 370–382.
- [7] A. Tiraferri, N.Y. Yip, A.P. Straub, S. Romero-Vargas Castrillon, M. Elimelech, A method for the simultaneous determination of transport and structural parameters of forward osmosis membranes, *J. Membr. Sci.*, 444 (2013) 523–538.
- [8] X. Chen, C. Boo, N.Y. Yip, Transport and structural properties of osmotic membranes in high-salinity desalination using cascading osmotically mediated reverse osmosis, *Desalination*, 479 (2020) 114335, doi: 10.1016/j.desal.2020.114335.
- [9] B. Kim, G. Gwak, S. Hong, Review on methodology for determining forward osmosis (FO) membrane characteristics: water permeability (*A*), solute permeability (*B*), and structural parameter (*S*), *Desalination*, 422 (2017) 5–16.
- [10] P. Xiao, L.D. Nghiem, Y. Yin, X.-M. Li, M. Zhang, G. Chen, J. Song, T. He, A sacrificial-layer approach to fabricate polysulfone support for forward osmosis thin-film composite membranes with reduced internal concentration polarisation, *J. Membr. Sci.*, 481 (2015) 106–114.
- [11] S.S. Manickam, J.R. McCutcheon, Understanding mass transfer through asymmetric membranes during forward osmosis: a historical perspective and critical review on measuring structural parameter with semi-empirical models and characterization approaches, *Desalination*, 421 (2017) 110–126.
- [12] N.Y. Yip, A. Tiraferri, W.A. Phillip, J.D. Schiffman, L.A. Hoover, Y.C. Kim, M. Elimelech, Thin-film composite pressure retarded osmosis membranes for sustainable power generation from salinity gradients, *Environ. Sci. Technol.*, 45 (2011) 4360–4369.
- [13] T.Y. Cath, A.E. Childress, M. Elimelech, Forward osmosis: principles, applications, and recent developments, *J. Membr. Sci.*, 281 (2006) 70–87.
- [14] M. Qasim, N.A. Darwish, S. Sarp, N. Hilal, Water desalination by forward (direct) osmosis phenomenon: a comprehensive review, *Desalination*, 374 (2015) 47–69.
- [15] G.D. Mehta, S. Loeb, Performance of permasep B-9 and B-10 membranes in various osmotic regions and at high osmotic pressures, *J. Membr. Sci.*, 4 (1979) 335–349.
- [16] T.Y. Cath, M. Elimelech, J.R. McCutcheon, R.L. McGinnis, A. Achilli, D. Anastasio, A.R. Brady, A.E. Childress, I.V. Farr, N.T. Hancock, J. Lampi, L.D. Nghiem, M. Xie, N.Y. Yip, Standard methodology for evaluating membrane performance in osmotically driven membrane processes, *Desalination*, 312 (2013) 31–38.
- [17] S.S. Manickam, J.R. McCutcheon, Model thin film composite membranes for forward osmosis: demonstrating the inaccuracy of existing structural parameter models, *J. Membr. Sci.*, 483 (2015) 70–74.
- [18] X. Zhang, L. Shen, W.Z. Lang, Y. Wang, Improved performance of thin-film composite membrane with PVDF/PFSA substrate for forward osmosis process, *J. Membr. Sci.*, 535 (2017) 188–199.
- [19] J. Ren, J.R. McCutcheon, A new commercial biomimetic hollow fiber membrane for forward osmosis, *Desalination*, 442 (2018) 44–50.
- [20] L. Xia, M.F. Andersen, C. Hélix-Nielsen, J.R. McCutcheon, Novel commercial aquaporin flat-sheet membrane for forward osmosis, *Ind. Eng. Chem. Res.*, 56 (2017) 11919–11925.
- [21] Y.-H. Pan, Q.-Y. Zhao, L. Gu, Q.-Y. Wu, Thin film nanocomposite membranes based on imolomite nanotubes blended substrates for forward osmosis desalination, *Desalination*, 421 (2017) 160–168.
- [22] X. Zhao, J. Li, C. Liu, A novel TFC-type FO membrane with inserted sublayer of carbon nanotube networks exhibiting the improved separation performance, *Desalination*, 413 (2017) 176–183.
- [23] S.-F. Pan, Y. Dong, Y.-M. Zheng, L.-B. Zhong, Z.-H. Yuan, Self-sustained hydrophilic nanofiber thin film composite forward osmosis membranes: preparation, characterization and application for simulated antibiotic wastewater treatment, *J. Membr. Sci.*, 523 (2017) 205–215.
- [24] X. Li, C. Heng, R. Wang, W. Widjajanti, J. Torres, Fabrication of a robust high-performance FO membrane by optimizing substrate structure and incorporating aquaporin into selective layer, *J. Membr. Sci.*, 525 (2017) 257–268.
- [25] C. Boo, Y.F. Khalil, M. Elimelech, Performance evaluation of trimethylamine-carbon dioxide thermolytic draw solution for engineered osmosis, *J. Membr. Sci.*, 473 (2015) 302–309.
- [26] S. Phuntsho, S. Hong, M. Elimelech, H. Kyong, Osmotic equilibrium in the forward osmosis process: modelling, experiments and implications for process performance, *J. Membr. Sci.*, 453 (2014) 240–252.
- [27] Z. Zhou, J.Y. Lee, T.-S. Chung, Thin film composite forward-osmosis membranes with enhanced internal osmotic pressure for internal concentration polarization reduction, *Chem. Eng. J.*, 249 (2014) 236–245.
- [28] T. Coleman, M.A. Branch, A. Grace, Optimization Toolbox For Use with MATLAB, The MathWorks, Inc., Natick, Massachusetts, USA, 1999.
- [29] J. Eddouibi, S. Abderafi, S. Vaudreuil, T. Bounahmidi, Water desalination by forward osmosis: dynamic performance assessment and experimental validation using MgCl₂ and NaCl as draw solutes, *Comput. Chem. Eng.*, 149 (2021) 107313, doi: 10.1016/j.compchemeng.2021.107313.
- [30] B. Yu, W. Hao, Levenberg–Marquardt Training, in: *Intell. Syst.*, 2011, CRC Press, Boca Raton, Florida, pp. 1–16.
- [31] G.N. Lewis, The osmotic pressure of concentrated solutions, and the laws of the perfect solution, *J. Am. Chem. Soc.*, 30 (1908) 668–683.
- [32] G.T. Gray, J.R. McCutcheon, M. Elimelech, Internal concentration polarization in forward osmosis: role of membrane orientation, *Desalination*, 197 (2006) 1–8.